MRS Advances © The Author(s), 2020, published on behalf of Materials Research Society by Cambridge University Press
DOI: 10.1557/adv.2020.422

Dry sliding wear of a Ni-based superalloy as a function of the aging time.

Luis E. Gonzalez A.[1], Arnoldo Bedolla-Jacuinde[1]*, Eduardo Cortés C, Francisco V. Guerra[1] and A, Ruiz[1]

[1]*Instituto de Investigaciones en Metalurgia y Materiales, Universidad michoacana de San Nicolás de Hidalgo, Morelia, Michoacán, México.*

**Corresponding author: abedollj@umich.mx*

Abstract. *From the present work, the wear behavior of aged Ni-based superalloy was analyzed under dry sliding conditions. Such alloy was melted in a vacuum induction furnace and cast into a ceramic mold. Then the alloy was solubilized at 1080ºC for 4 hours and then aged at 760ºC for 4, 8, 16, 24, 48, 72 and 150 hours. The alloy was characterized as-cast and also in the heat-treated conditions by transmission electron microscopy (TEM), scanning electron microscopy (SEM) and X-ray diffraction (XRD). Mechanical characterization included just Vickers hardness and wear resistance under dry sliding conditions by a block on ring configuration according to the ASTM G77 standard. Wear tests were undertaken for 2000 m at a speed of 0.7 ms^{-1} at two different loads (25 and 78 N). The worn samples were analyzed by an optical profiler to determine the wear volume and by SEM to analyze the worn surface and the microstructure below the worn surface. The main findings indicate the formation of an oxide layer mainly formed by Cr and Ni during sliding. The thickness of such a layer is about 10 μm for short aging times and about 5 μm for longer aging times. For this load, the wear resistance was 50% higher for the shorter aging times than that for the longer aging times. This behavior is described in terms of the thickness of the protecting layer, and on the availability of chromium to form such a layer since it forms $Cr_{23}C_6$ at long aging times. On the other hand, for a load of 78 N the wear behavior is in agreement with hardness. Wear resistance increases with aging time due to the higher precipitation of prime gamma phase.*

1. INTRODUCTION

Nowadays the use of clean energy is of great importance for the future of a better tomorrow. The most used alloys for this purpose are titanium-, aluminum-, and nickel-based alloys. This later group of alloys is widely used for several components in turbines, either for gas-, carbon, or steam turbines. The main reason why these alloys are degraded by the normal use, is due to the high temperatures they are commonly subjected, above 600 ° C. Some of the pieces made of superalloys are blades, disc turbines and rotors, etc. Blades and discs are the components that undergo the most wear and the highest temperatures. The most significant wear mechanism observed in superalloys is oxidative and erosive, particularly in components such as blades. Research works have tried to attack this problem through the application of thermal barriers on the areas that lead to higher wear, they have also modified the design of turbines in order to reduce the aggressive flow, etc. [1-3]. Some nickel-based alloys such as Waspaloy and Udimet are commonly used in rotors due to their good corrosion and creep resistance, however, these alloys experience wear during sliding. Under these conditions, the metal-metal contact is accompanied by vibration, which impairs the operation and accelerates wear. This kind of vibration is impossible to reduce in certain regions, for example in the supports of the turbines and particularly in tubes [4]. The wear by sliding contact is characterized by the elimination of material from two contacting surfaces under relative motion due to the friction on both surfaces [5, 6]. The degradation of the surface and the microstructure below the worn surface involve complex wear processes, which in turn determine the wear phenomena that contribute to the loss of material. The most commonly observed phenomena that contributed on wear in these alloys are: tribochemical reaction, plastic deformation and cracking [7, 8]. These phenomena depend on the sliding conditions, and it has been reported that for soft sliding conditions, cracking and adhesive wear commonly occur; and that for severe conditions, wear occurs by oxidation, delamination and abrasion [9-12]. From the present work, oxidation was the main wear mechanism observed.

2. EXPERIMENTAL PROCEDURE

The alloy under study was melted in a vacuum induction furnace (VIP-CONSARC). The melting was carried out at a temperature of 1600 ° C and cast into a ceramic molds. The obtained ingots were sectioned for characterization in the as-cast conditions and for a subsequent heat treatment. The alloy was solubilized at 1080 ° C for 4 hours followed by air-cooling to room temperature. Subsequently, a stabilization heat treatment was carried out at 850 ° C for 24 h and air cooled to room temperature. Finally, the material was aged at 760 ° C to precipitate the γ´ phase. The aging times were 4, 8, 16, 24, 48, 72 and 150 hours, followed by air-cooling. Metallographic analysis was done in a traditional way, grinding on abrasive paper and polishing on nylon cloth with diamond paste as the abrasive. Samples were then electro-polished on a Lectropol-5 Struers equipment using an electrolyte composed of 10% perchloric acid and 90% methanol, at 30 V for 60 s. Etching was carried out with Marble´s reagent (10 gr $CuSO_4$, 50 ml HCl, and 50 ml distilled water) for 20 s to reveal the microstructure. The characterization was undertaken by optical microscopy (MO), SEM at 20 kV for imaging and EDS for microanalysis. Hardness tests were undertaken in a Vickers Hardness Tester by using a load of 30 Kg for 10 s. Finally, the sliding wear test were carried out on the block on ring configuration. The superalloy was tested for wear in both as-cast and heat-treated

conditions. The tests were carried out without lubrication (dry), for a constant distance of 2000 meters at 0.7 ms^{-1} under loads of 25 and 78 Newton (N), and using a ring of a hardened M2 steel (62 HRC). The specimens for wear were rectangular blocks of 1x1x1.5 cm polished on the contact surface with 1 μm diamond paste. A NANOVEA Sp50 optical profiler was used to digitalize the topography of the worn surface and to measure the volume lost after each test. Finally, the worn surfaces were analysed by scanning electron microscopy and X-ray diffraction was used to characterize the wear debris.

3. RESULTS

3.1 microstructure

Table I shows the chemical composition of the Ni base superalloy. The contents of Ti and Al promote the precipitation of γ' phase. The high chromium content (20.5%) gives good corrosion resistance to the alloy, and as will be discussed later, it plays an important role on the wear resistance. Figure 1 shows SEM micrographs of the general view of the structure of the aged alloy for 8 h (Fig 1a), and detail of the grain boundary and a MC carbide (Fig 1b). MC carbides, mainly composed by titanium, are present always in the alloy and do not dissolve during the solubilisation heat treatment. During aging, it is common the precipitation of $Cr_{23}C_6$ at grain boundaries as can be observed from these micrographs. Figure 2 shows also SEM micrographs giving detail of MC carbides (TiC and TiMoC) of the alloy aged for 4h (Fig 2a) and for 48 h (Fig 2b). Note the presence of γ´ (Ni_3(Al Ti)) precipitates in the γ matrix.

Table I Nominal compositions of alloys in wt. %.

Cr	Co	Mo	Al	Ti	V	C	Fe	Zr	Ta	B	Ni
20.5	13.6	5.03	1.57	3.42	0.115	0.15	1.64	0.07	0.24	0.01	Bal

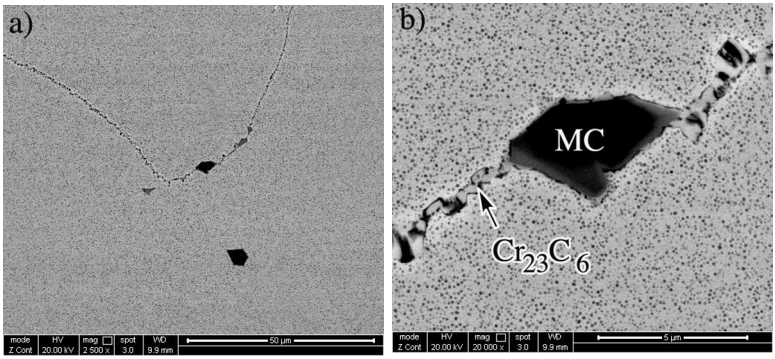

Figure 1. Backscattered electron micrographs showing the structure of the experimental alloy aged for 8 h. a) general, and b) detail of grain boundary.

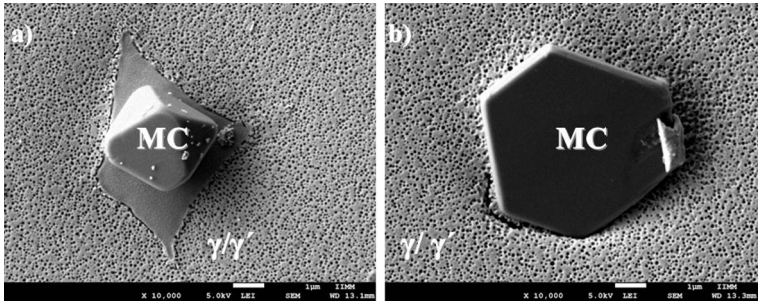

Figure 2 Scanning micrographs showing the γ' precipitates in the matrix. The primary MC carbides formed by Ti are also observed. a) 4 h and b) 48 h.

The aim of the aging heat treatment is to obtain the maximum precipitation of γ´ within the matrix, and for the present study, after 48 h aging a saturation of γ´ was observed in the matrix. For aging times of 72 h or more, precipitation hardly increases and for the aging times of 150 hours, over-aging was observed. Figure 3 shows hardness as a function of the aging time; note the maximum hardness for the 72 h heat treatment. For longer aging times, in addition to the precipitation of γ´, $M_{23}C_6$ precipitation at grain boundaries occurred, also the precipitation of TCP phases and a small surface degradation of the MC carbides were observed (Figure 4). These phenomena in over-aged alloys may contribute in a negative way in the wear behavior of the alloy. Figure 4 shows the microstructure of the alloy aged for 150 h; note the presence of brittle TCP phases.

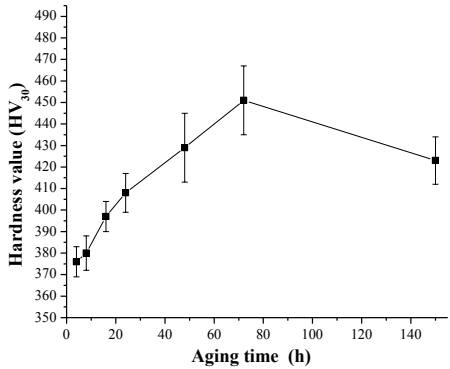

Figure 3. Hardness as a function of aging time for the experimental alloy.

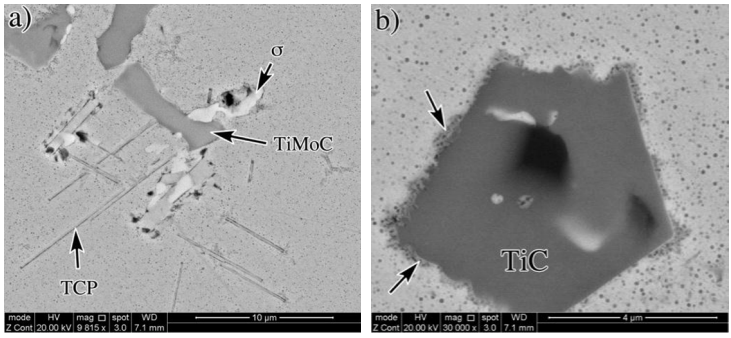

Figure 4. Electron backscattered micrographs showing detail of the phases present for the alloy aged for 150 h (overaged); a) the presence of sigma and TCP phases, and b) detail of the partial dissolution of the surface of a TiC.

3.2 Wear Behavior

Figure 5 shows an example of the non-contact profiler study. The wear track was digitalized and the volume lost was easily measured for all the samples after the wear tests. Figure 6 shows the wear volume lost (as measured from the profiler studies) as a function of the aging time for the two applied loads.

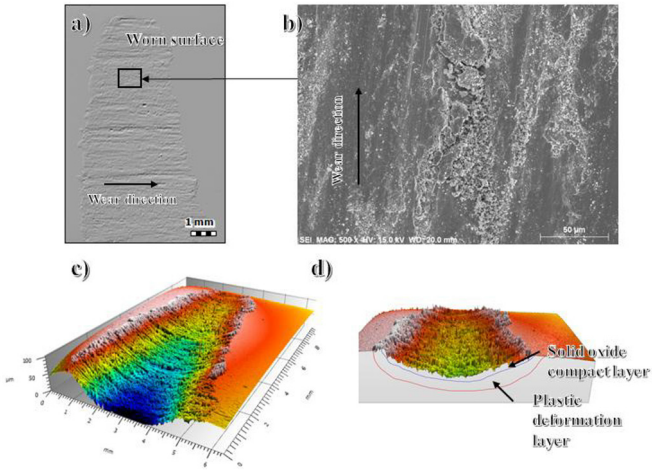

Figure 5. Non-contact profiler analysis of the worn surface. Sample tested at 78 N.

The wear behavior was different for each load. For the case of the 25 N applied load, the volume lost after the test goes from 0.45 mm^3 for the alloy aged for 4 h to 0.75 mm^3 for the alloy aged for 24 h. For longer aging times, the wear volume seems to be constant 0.75 mm^3; no notorious change was observed. As mentioned previously, the main wear mechanism observed during the wear test was oxidative. This implies the formation of an oxide layer on the surface of the alloy. The rate at which the oxide layer is formed and detached represents the wear rate [13].

According to the plot, the wear volume lost is lower for low aging times when the applied load is 25 N; this can be explained by the stability of the oxide layer protecting

the surface. For the wear tests undertaken at this particular load, a thicker oxide layer was observed for low aging times (between 5 and 7 μm thickness) than that observed for aging times of 24 h or longer (about 2 or 3 μm thickness). Figures 7 shows cross sections of the alloy aged for 4 h and the alloy aged for 24 h. Note the thickness of the oxide layer. Similarly, figure 8 shows the worn surface of the alloys aged for 4 and 24 h respectively. Note from this later figure, the smoother compact layer formed for the alloy aged for 4h and the rough surface of the alloy aged for 24 h. Such a difference in oxide appearance and thickness is clear evidence of the protective effect against friction that the oxide layer provides to the alloy as the wear test progresses.

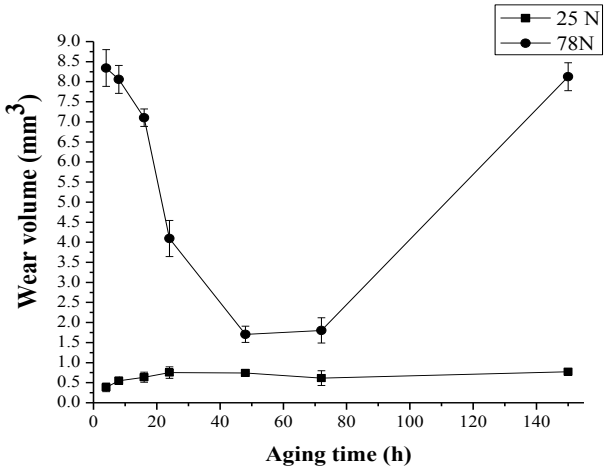

Figure 6. Volume lost as a function of the aging time.

The development of a thin oxide layer provides low lubricating contact and such a layer detaches more easily than a thick layer. Friction coefficients measured during the wear tests indicate values between 0.3 and 0.4 for the low aging times, and between 0.5 and 05 for the tests on the alloys aged or more than 24 h. It is assumed that for low aging times, higher amounts of chromium are available to form the oxide layer [14]; such an stable chromium-rich layer has good adherence to the substrate and gets thicker before detaching. On the other hand, for the alloys aged for times longer than 24 h, less chromium is available since the precipitation of large amounts of $Cr_{23}C_6$ has occurred. In addition, the presence of TCP phases also consume chromium and molybdenum, and the presence of these brittle phases may reduce the adherence of the oxide layer; such a layer, then detaches easily when is still thin.

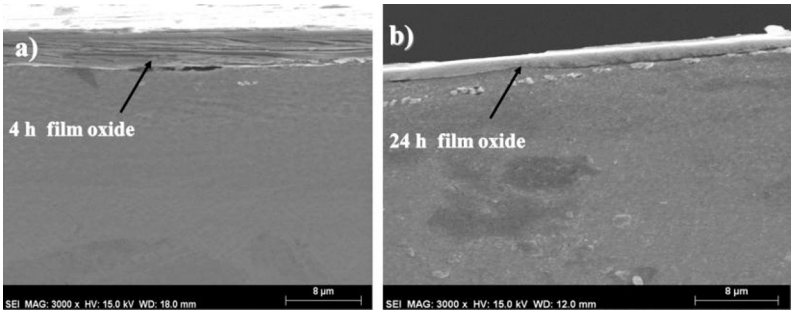

Figure. 7 Cross section SEM micrograph showing the oxide layer theickness after the wear test of the experimental alloy tested at 25 N and aged for a) 4 h and b) 24 h.

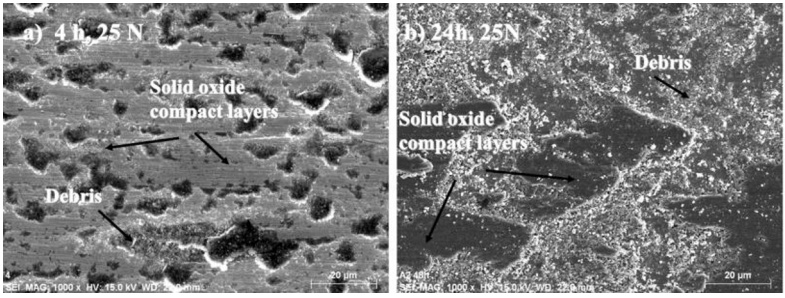

Figure 8. SEM micrographs of the worn surface after the wear test of the experimental alloy tested at 25 N and aged for a) 4 h and b) 24 h.

The stability of chromium oxide rich protective layers formed in nickel- and cobalt-based superalloys has been reported by H. Stott et. al. [15]. They report that the formation of such an oxide layer forms more easily in the Ni alloy than in the Co alloy and conclude that the presence of chromium as an oxide gives more protection against friction at any temperature due to the stability of the oxide.

For the present work, the detailed characterization of the oxide layer was out of the scope. However, based on the work of J. Glascott [16]; it is known that in Ni based alloys, thin layers of NiO, Cr_2O_3, Co_3O_4, and $NiCr_2O_4$, oxides are formed, and that the film undergoes plastic deformation during the sliding, forming a smooth surface that reduces friction.

Figure 9 shows a cross section of one of the samples tested at 25 N and aged for 4 h, and the chemical microanalysis obtained from the oxide layer. As can be seen, the oxide layer is mainly formed by chromium, nickel, molybdenum, titanium and aluminum. Further characterization by XRD on the wear debris collected after the tests indicate they are composed by Cr_2O_8, NiO, Fe_2O_3, TiO and Al_2O_3 as shown from figure 10.

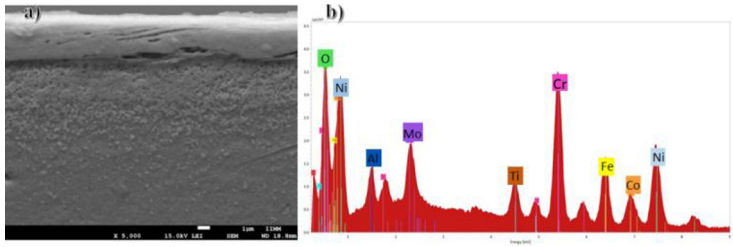

Figure 9. SEM micrograph showing the oxide layer on the worn surface and its respective EDS.

Due to the high chromium content, most superalloys exhibit good corrosion resistance due to the natural oxide layer developed at the surface [14, 17, 18]. This oxide layer also avoids the direct metal-metal contact during sliding under low or moderate loads. As mentioned before, the Cr_2O_3 oxide layer is the most stable and protective film. To maintain the continuous formation of such an oxide it is necessary to have enough chromium at the surface, other way, elements such as iron, molybdenum, nickel, etc, will oxidize to compensate the lack of chromium. This will result in the increase of the oxidation rate and in turn in the wear rate.

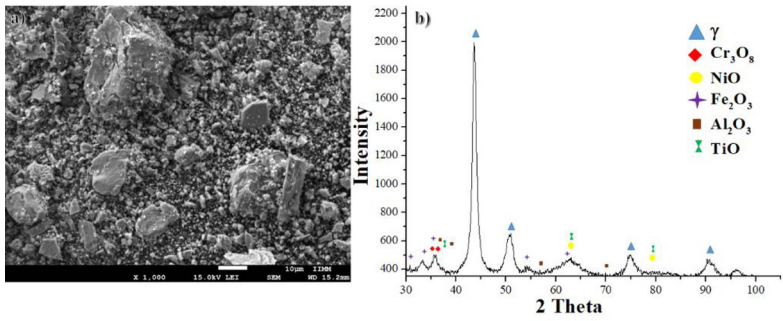

Figure 10. Wear debris obtained after the wear test undertaken at 25 N for the alloy aged for 4 h and its respective X-ray diffraction pattern.

For the case of the alloy tested at 78 N (figure 6), the volume lost for the aging time of 4 h is about 8.5 mm^3 and it decreases to 1.75 mm^3 for the aging times of 48 and 76 h. For longer aging times (150 h) the volume lost increased to 7.5 mm^3. The decrease in wear is in agreement with hardness (figure 3). Maximum hardness was obtained for the alloy aged for 76 h. For these wear tests at low aging times the thickness of the oxide layer was between 2 and 3 μm. These thin layers along with severe plastic deformation are considered to be the main responsible for the low wear resistance. Low aging times indicates low hardness values; therefore, more plastic deformation below the worn surface is experienced by the severe stresses during the surfaces sliding (see figure 11). When severe plastic deformation of the substrate below the worn surface, an easy detachment of the brittle oxide layer occurs and the wear rate increases [19, 20].

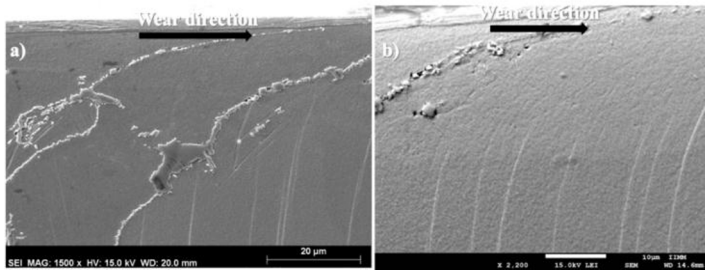

Figure 11 Cross sections of the alloys tested at 78 N and aged for: a) 4 h and b) 8 h. Note the plastic deformation below the worn surface and the thin oxide layer.

The thickness of the oxide layer for the alloys tested at 78 N and aged for 48 and 76 h, shown values between 8 and 10 µm. For these maximum hardness alloys, plastic deformation is much less, therefore the oxide layer remains attached to the substrate for longer times and it gets thicker for the same reason. Such a thick layer diminishes friction during sliding and the wear rate is then lower. Figure 12 shows SEM micrographs of the structure below the worn surface, where the low deformation and thicker oxide layers are observed for the alloys aged at 48 and 76 h. Note the presence of some cracks (arrowed) of the TiMoC carbides below the worn surface. The presence of a large number of nanometric precipitates homogeneously distributed, provides the matrix with a better wear resistance since the high hardness value diminishes plastic deformation below the worn surface. Some works on high-chromium white irons [21, 22] have reported less wear resistance when the austenitic matrix flows plastically and the eutectic carbides are fractured. In Ni base superalloys, the γ′ precipitates decrease the plastic deformation in the matrix by decreasing the movement of dislocations; and in turn decreasing the development of cracks on the brittle phases (MC, TCP and $Cr_{23}C_6$).

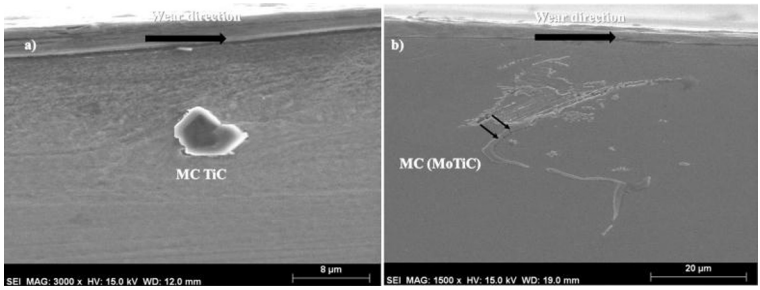

Figure 12. SEM micrographs showing the structure below the worn surface for the alloys testes at 78 N and aged for: a) 48 h and b) 76 h.

For the case of the overaged alloy (aged for 150 h) wear resistance decreased drastically. This is explained in terms of the presence of high amounts of the brittle phases mentioned before. The overaged alloy experiences high plastic deformation below the worn surface which transfer high stresses to the brittle phases, which are prone to crack. Figure 13 shows two cross sections of the alloy tested at 78 N and aged for 150 h; note the

flow of the matrix and the bending of the brittle TCP phase. The TCP phases have been reported to be deleterious for creep [23, 24] and also for wear resistance due to their brittle nature.

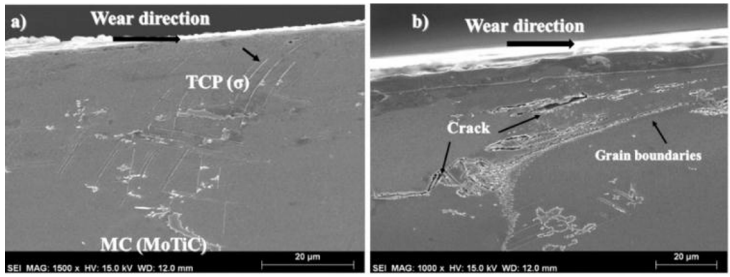

Figure 13. SEM micrographs showing TCP phase alignment with the direction of wear.

CONCLUSIONS

The wear behavior of the alloy was different for each applied load.

For the wear tests at 25 N, the main wear mechanism was oxidative. An oxide layer was developed on the rubbing surface, such a layer increased in thickness and then got detached. The lower wear was observed for the alloys aged up to 16 h and was attributed to the formation of a stable chromium oxide layer. For longer aging times, high precipitation of chromium carbides occurred, which reduced the amount of chromium to form the oxide layer during the wear tests.

For the wear at 78 N, also oxidative wear occurs, particularly for the alloys aged for times up to 76 h. Wear resistance increased with aging time up to 76 h aging. The hardening effect of γ' during aging contributed to the development of a stable thick oxide layer. On the contrary, for the overaged alloy (150 h aging) large metallic debris were detached due to the presence of brittle phases developed at this aging time. Cracks initiated at grain boundaries and at the brittle TCP phases; this destabilized the subsurface of the alloys.

ACKNOWLEDGMENTS

This research work was developed under the financial support of the Mexican Center for Geothermal Energy (CeMIE-Geo) under the grant No: 019. The authors are very grateful to The Department of Energy of Mexico (SENER) and the National Council of Science and Technology of Mexico (CONACyT) for the sponsorship. Two of the authors, Luis Gonzalez and Eduardo Cortés, also acknowledge the CONACyT for the scholarship during their Ph.D.

REFERENCES

[1] Hardwicke, C.U. and Y.-C. Lau, Advances in Thermal Spray Coatings for Gas Turbines and Energy Generation: A Review. Journal of Thermal Spray Technology, 22(5) (564-576) 2013.

[2] Tawancy, H.M. and L.M. Al-Hadhrami, Comparative performance of turbine blades used in power generation: Damage vs. microstructure and superalloy composition selected for the application. Engineering Failure Analysis, 46 (76-91) 2014.

[3] Stoyanov, P., Dawan L., Goberman D., and Shah D., Friction and Wear Characteristics of Single Crystal Ni-Based Superalloys at Elevated Temperatures. Tribology Letters, 66(1) (47-52) 2018.

[4] Xin L., Yang B., Wang Z., Li J., Lu Y., and Shoji T., Effect of normal force on fretting wear behavior and mechanism of Alloy 690TT in high temperature water. Wear, 368-369 (210-218) 2016.

[5] Xin L., Yang B., Wang Z., Li J., Lu Y., and Shoji T.,, Microstructural evolution of subsurface on Inconel 690TT alloy subjected to fretting wear at elevated temperature. Materials & Design, 104 (152-161) 2016.

[6] Benea, L., Basa S., Danaila E., Caron N., Raqquet O., Ponthioux P., and Celis J.P., Fretting and wear behaviors of Ni/nano-WC composite coatings in dry and wet conditions. Materials & Design (1980-2015), 65 (550-558) 2015.

[7] Chung, I. and M. Lee, An experimental study on fretting wear behavior of cross-contacting Inconel 690 tubes. Nuclear Engineering and Design, 241(10) (4103-4110) 2011.

[8] Li, J., Lu Y., Zhang H., and Xin L., Effect of grain size and hardness on fretting wear behavior of Inconel 600 alloys. Tribology International, 81 (215-222) 2015.

[9] Heredia, S. and S. Fouvry, Introduction of a new sliding regime criterion to quantify partial, mixed and gross slip fretting regimes: Correlation with wear and cracking processes. Wear, 269(7) (515-524) 2010.

[10] Wang, Z.H., Lu Y.H., Li J., and Shoji T., Effect of pH value on the fretting wear behavior of Inconel 690 alloy. Tribology International, 95 (162-169. 2016.

[11] Thirugnanasambantham, K.G. and S. Natarajan, Mechanistic studies on degradation in sliding wear behavior of IN718 and Hastelloy X superalloys at 500°C. Tribology International, 101(324-330) 2016.

[12] Mi, X., Cai Z., Xiong X., Qian H., Tang L., Xie Y., Peng J., and Zhu M., Investigation on fretting wear behavior of 690 alloy in water under various temperatures. Tribology International, 100 (400-409) 2016.

[13] Okazaki, M., High-temperature strength of Ni-base superalloy coatings. Science and Technology of Advanced Materials, 2(2) (357-366) 2001.

[14] Andrieu, E., Molins R., Ghonem H., and Pineau A., Intergranular crack tip oxidation mechanism in a nickel-based superalloy. Materials Science and Engineering: A, 154(1) (21-28) 1992.

[15] H. Stott, F., C. W. Stevenson, and G. C. Wood, Friction and wear properties of Stellite 31 at temperatures from *293 to 1073K*. Metals and Technology, 4 (66-74) 1977.

[16] Glascott, J., F.H. Stott, and G.C. Wood, The effectiveness of oxides in reducing sliding wear of alloys. Oxidation of Metals, 24(3) (99-114) 1985.

[17] Wang, J., Zhou L., Sheng L., and Guo J., The microstructure evolution and its effect on the mechanical properties of a hot-corrosion resistant Ni-based superalloy during long-term thermal exposure. Materials & Design, 39 (55-62) 2012.

[18] Sidhu, T.S., S. Prakash, and R.D. Agrawal, Hot corrosion and performance of nickel-based coatings. Current Science, 90(1) (41-47) 2006.

[19] Sauger, E., Ponsonnet L., Martin J.M., and Vincent L., Study of the tribologically transformed structure created during fretting tests. Tribology International, 33(11) (743-750) 2000.

[20] Zhou, Z.R., Sauger E., Liu J.J., and Vincent L., Nucleation and early growth of tribologically transformed structure (TTS) induced by fretting. Wear, 212(1) (50-58) 1997.
[21] Bedolla-Jacuinde, A., Guerra F.V., Mejia I., Zuno-Silva J., and Rainforth M., Abrasive wear of V–Nb–Ti alloyed high-chromium white irons. Wear, 332-333 (1006-1011) 2015.
[22] Cortés-Carrillo, E., Bedolla-Jacuinde A., Mejia I., Zepeda C.M., Zuno-Silva J., and Guerra-Lopez F.V., Effects of tungsten on the microstructure and on the abrasive wear behavior of a high-chromium white iron. Wear, 376-377 (77-85) 2017.
[23] Holt, R.T. and W. Wallace, Impurities and trace elements in nickel-base superalloys. International Metals Reviews, 21(1) (1-24) 1976
[24] Qin, X.Z., Guo J.T., Yuan C., Chen C.L., and Ye H.Q., Effects of Long-Term Thermal Exposure on the Microstructure and Properties of a Cast Ni-Base Superalloy. Metallurgical and Materials Transactions A, 38(12) (3014-3022). 2007.